Experimental Realization of Multi-ion Sympathetic Cooling on a Trapped Ion Crystal

Z.-C. Mao[1,*] Y.-Z. Xu,[1,*] Q.-X. Mei,[1] W.-D. Zhao,[1] Y. Jiang,[1] Y. Wang,[2,†] X.-Y. Chang,[1] L. He,[1] L. Yao,[1] Z.-C. Zhou,[1,3,‡] Y.-K. Wu,[1,§] and L.-M. Duan[1,∥]

[1]Center for Quantum Information, Institute for Interdisciplinary Information Sciences, Tsinghua University, Beijing 100084, People's Republic of China
[2]School of Physics, Peking University, Beijing 100871, People's Republic of China
[3]Beijing Academy of Quantum Information Sciences, Beijing 100193, People's Republic of China

Trapped ions are one of the leading platforms in quantum information science. For quantum computing with large circuit depth and quantum simulation with long evolution time, it is of crucial importance to cool large ion crystals at runtime without affecting the internal states of the computational qubits, thus the necessity of sympathetic cooling. Here, we report multi-ion sympathetic cooling on a long ion chain using a narrow cooling beam focused on two adjacent ions, and optimize the choice of the cooling ions according to the collective oscillation modes of the chain. We show that, by cooling a small fraction of ions, cooling effects close to the global Doppler cooling limit can be achieved. This experiment therefore demonstrates an important enabling step for quantum information processing with large ion crystals.

Owing to the long coherence time [1], convenient optical initialization and readout [2], as well as the accurate laser [2–5] and microwave [6–9] control, the trapped ion system has demonstrated single-qubit-gate fidelity of 99.9999% [10], two-qubit-gate fidelity above 99.9% [11,12], multi-ion Greenberger-Horne-Zeilinger (GHZ) entangled states with up to 24 ions [13], quantum error correction using 13 ions [14], and global quantum simulation of 53 ions in a Paul trap [15] and up to hundreds of ions in a Penning trap [16,17]. These make ion trap a leading candidate for quantum information processing.

Motional heating is one of the major limiting factors for the application of trapped ions caused by, e.g., electric field noise [18,19] and collision with background gas molecules [18]. While the Mølmer-Sørensen gate [20,21], a widely used two-qubit entangling gate scheme for trapped ions, does not require ground state cooling of the motional states, heating during the gate operation does lead to decoherence. Besides, too high a temperature can also result in the breakdown of the Lamb-Dicke approximation [2] which requires that ions' oscillation amplitudes be much smaller than the laser wavelength. This will thus have considerable contribution to the gate infidelity. For larger ion crystals, the heating effect becomes more significant and can further influence the stability of the crystal [22], thereby prevents large-scale ion trap quantum simulation with long evolution time, or quantum computing circuits with large depth. Finally, while current schemes for ion trap quantum computing mainly consider one-dimensional (1D) ion chains and utilize additional ion shuttling [18,23] or photonic quantum network [24–26] techniques to scale up, proposals also exist to directly use large 2D or 3D ion

crystals [27,28], for which the motional heating can be even more severe. Therefore, it is necessary to introduce cooling mechanisms at runtime to compensate the heating effect.

The commonly used laser cooling methods such as the Doppler cooling [2], electromagnetically-induced-transparency cooling [2,29,30], polarization gradient cooling [31], and resolved sideband cooling [2] all exploit the transitions among the internal atomic levels, thus are generally unsuitable for the runtime protection of the ionic qubits. For this purpose, sympathetic cooling can be used where a fraction of the ions can be chosen as ancillae (cooling ions) to cool the other ions (computational ions) through their mutual Coulomb interaction, in such a way that the standard laser cooling on the cooling ions with spectral or spatial selection will not affect the internal states of the computational ions. Previous experimental demonstrations of sympathetic cooling mainly consider small ion crystals [32–37]. For larger ion crystals the sympathetic cooling generally becomes inefficient unless the multi-ion collective oscillation modes are carefully taken into account [38], which has not yet been demonstrated experimentally.

In this Letter, we report the first multi-ion sympathetic cooling experiment on a long ion chain, where collective modes have to be considered when choosing the cooling ions. We propose a convenient yet efficient scheme to cool a few adjacent ions at optimized locations and demonstrate that, by cooling only two ions in a long chain of 8 to 28 ions, the whole crystal can be cooled efficiently to near the global Doppler cooling limit. Our scheme can be generalized to larger 2D or 3D crystals and will play a critical role in their runtime stabilization for future large-scale ion trap quantum computing and simulation.
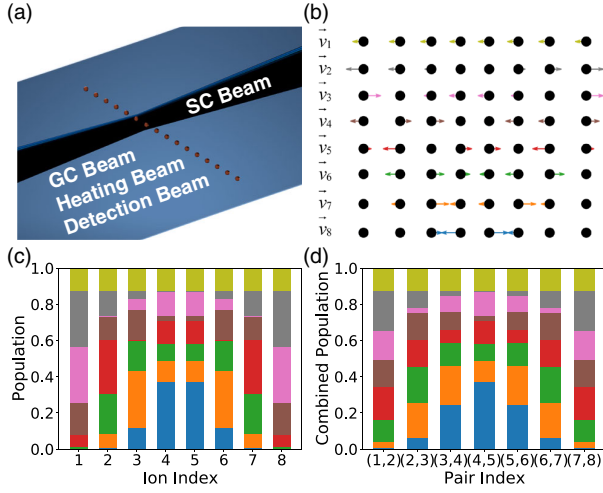
FIG. 1. (a) Schematic experimental setup. A broad beam is applied to all the ions for global cooling (GC), detection or heating, by varying its frequency components and intensity in the time sequence. A narrow sympathetic cooling (SC) beam is used to cool the selected ion pairs. (b) Graphical illustration of the eight axial normal modes for a chain of $N = 8$ ions. (c) The relative population (squared relative amplitudes) of each ion in each mode. A reflection symmetry over the chain can be observed. Different colors represent different normal modes as appearing in (b). A "missing" color for an ion indicates a vanishing mode population. As can be seen, no single ion can have large population in all the modes. (d) The relative population of two adjacent ions (their sum with a further normalization) in each mode. In this case the pairs (2, 3), (3, 4), (5, 6), and (6, 7) have a visible population in all the modes.

Our experimental setup is sketched in Fig. 1(a). We use a four-rod Paul trap with a transverse trap frequency $\omega_x = 2\pi \times 1.048$ MHz and an axial trap frequency $\omega_z = 2\pi \times 81$ kHz to hold ^{174}Yb$^+$ ions in a linear configuration. A broad laser beam covering all the ions is applied at an angle of 45° from the axial direction for global Doppler cooling, detection, and heating of the ions. A narrower sympathetic cooling beam propagates in the opposite direction to address the desired ions. Both the axial and the transverse modes can be cooled or heated by these laser beams, but only the axial oscillations are measured owing to the larger amplitudes. The discussion about the transverse modes is placed in Supplemental Material [39] and more details about the setup can be found in Ref. [22].

The dynamics of an ion chain with ion mass m in a harmonic trap $V(x, y, z) = \frac{1}{2}m(\omega_x^2 x^2 + \omega_y^2 y^2 + \omega_z^2 z^2)$ with cooling and background heating can be described by the Heisenberg-Langevin equations [38]

$$\dot{p}_i^\xi = -\sum_j A_{ij}^\xi x_j^\xi - \gamma_i^\xi p_i^\xi + \sqrt{2\gamma_i^\xi}\zeta_i^\xi(t), \qquad (1)$$

where $i, j = 1, \ldots, N$ indicate each ion and $\xi = x, y, z$ for each spatial direction, and $\dot{p}_i^\xi$ is the time derivative of the

momentum p_i^ξ of ion i in direction ξ. Near the linear equilibrium configuration the motions for different ξ are decoupled. The trapping force and the Coulomb interaction are described by the matrix A^ξ, whose elements are $A_{ii}^\xi = m\omega_\xi^2 - (e^2/4\pi\varepsilon_0)\sum_{j\neq i}(C^\xi/|z_{0,j} - z_{0,i}|^3)$ and $A_{ij}^\xi = (e^2/4\pi\varepsilon_0)(C^\xi/|z_{0,j} - z_{0,i}|^3)$ $(i \neq j)$, where $z_{0,i}$ represents the equilibrium positions of the ions in the axial direction and $C^{x,y} = 1$, $C^z = -2$.

In the second term of Eq. (1), the damping rate γ_i^ξ or cooling rate for an ion under Doppler laser cooling is $\gamma_0 = -(8\hbar k^2/m)(\Delta/\Gamma)(s/2/[1 + s + (2\Delta/\Gamma)^2]^2)$ [2], where k is the wave number of the cooling laser projected to a principal axis, Γ the spontaneous emission rate, Δ the laser detuning, and s the saturation parameter. The last term describes a random force on the ions. For the ions being laser cooled, we simply have $\langle\zeta_i(t)\zeta_j(t')\rangle = \delta_{ij}\delta(t - t')mk_BT_D$, where $T_D \sim \hbar\Gamma\sqrt{1 + s}/k_B$ is the Doppler cooling limit. As for the background heating, here we follow Ref. [38] to assume independent thermal baths for individual ions, that is, $\langle\zeta_i(t)\zeta_j(t')\rangle = \delta_{ij}\delta(t - t')mk_BT_{bg}$. Later we will also consider the case where the background heating is correlated for different ions. Assuming an environment temperature $T_{bg} = 300$ K and a background heating rate $\kappa = 50$ mK/ s (about 1000 phonons per second in the transverse mode), the corresponding damping rate is $\gamma_i^\xi = \kappa/T_{bg} = 1.67 \times 10^{-4}$ Hz and is negligible compared with γ_0 for the ions being cooled.

We use the position fluctuation $\delta z_i \equiv \sqrt{\langle\delta z_i^2\rangle}$ and its average over the ion chain $\overline{\delta z}$ to quantify the cooling effect [38], which can be computed analytically from Eq. (1) (see Supplemental Material [39]). Throughout this Letter, we use brackets to denote ensemble average of the thermal baths and use overlines for the average over the chain. Reference [38] suggests that the effect of sympathetic cooling may be related to the normal mode population of the ions being cooled. As we can see in Figs. 1(b)–1(d), no single ion can have a large population in all the modes, while combining just two ions gives a much larger population. Inspired by this observation, as well as the experimental convenience of using just one narrow cooling beam, in Fig. 2(a) we consider the sympathetic cooling using one, two, three, and four adjacent ions and compute the average position fluctuation for a chain of $N = 121$ ions. In general, cooling a single ion gives large axial position fluctuation, while cooling two or more optimized adjacent ions can result in nearly the same cooling limit as the global Doppler cooling.

To further showcase the intrinsic correlation between the sympathetic cooling effect and the normal mode population, we define an indicator $CP_{min}^{(n)}(i)$, which is the minimum over all the N axial modes for the combined normal mode population of n adjacent ions centered at ion i. For

example, $\mathrm{CP}_{\min}^{(2)}(i)$ is the shortest vertical bar for each pair in Fig. 1(d). Since the total population over all the modes is normalized, the larger the minimum, the more uniform the distribution is. As we can see in Fig. 2, the region with high $\mathrm{CP}_{\min}^{(n)}(i)$ does coincide with a strong sympathetic cooling effect. We can thus use $\mathrm{CP}_{\min}^{(n)}(i)$ as a convenient criterion to choose the optimal cooling beam location. For this $N = 121$ ion chain, we thereby choose the ion pair (55, 56) and compare the axial position fluctuation δz_i for the optimal sympathetic cooling with that for global Doppler cooling in Fig. 2(c). The position fluctuation is nearly identical for the two cases around the center, and even for ions on the edges, the difference is less than 30%, which indicates efficient sympathetic cooling using only two out of 121 ions. Incidentally, here we get a symmetric distribution of δz_i under an asymmetric cooling configuration. This originates from the reflection symmetry in the normal modes and the fact that the energy propagation on the chain is faster than the cooling and the heating process.

Now we study the multi-ion sympathetic cooling of an ion chain in the experiment and explore the influence of the cooling beam location. As shown in Fig. 3(a), we start from an $N = 16$ ion chain in the global Doppler cooling limit and heat it by a global heating beam at about 20 μW for

5 ms. Then we turn on a 30 nW sympathetic cooling beam at various positions for various duration and finally detect the fluorescence of the ions to fit the FWHMs of a multipeak Gaussian function. Under a fixed imaging system, the fitted width (which we also denote as δz_i) will be positively correlated to the axial position fluctuation and thus can reflect the temperature of the ions. The measured evolution of $\overline{\delta z}(t)$ is shown in Fig. 3(b) for two ions on the edge, in (c) for the optimal location, and in (d) for two ions at the center. Since the ion separation is not uniform over the chain, we carefully calibrate the cooling beam profile to keep the laser intensity identical on different ion pairs for a fair comparison (see Supplemental
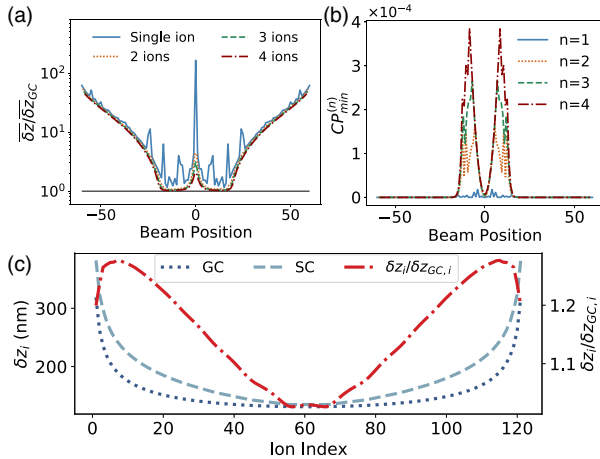

FIG. 2. (a) The theoretical cooling limit by cooling one to four adjacent ions at various positions of an $N = 121$ ion chain with $\omega_{x,y} = 2\pi \times 5$ MHz and $\omega_z = 2\pi \times 0.05$ MHz. We set $\gamma_0 = 26$ kHz, $T_D = 3$ mK, $\kappa = 50$ mK/ s, and $T_{bg} = 300$ K. The cooling effect is characterized by the average position fluctuation $\overline{\delta z}$ of all the ions in the axial direction and is further normalized by that of global Doppler cooling (the black horizontal line). The horizontal axis represents the beam position with each ion labeled from $-(N-1)/2$ to $(N-1)/2$. (b) Our simplified criterion $\mathrm{CP}_{\min}^{(n)}$ for $n = 1, 2, 3, 4$. Higher $\mathrm{CP}_{\min}^{(n)}$ indicates better cooling effects. (c) The axial position fluctuation δz_i of each ion when sympathetically cooling the optimal ion pair (55,56) (SC) using the criteria of (b) and the corresponding curve for global Doppler cooling (GC). The red dash-dotted line shows their ratio.
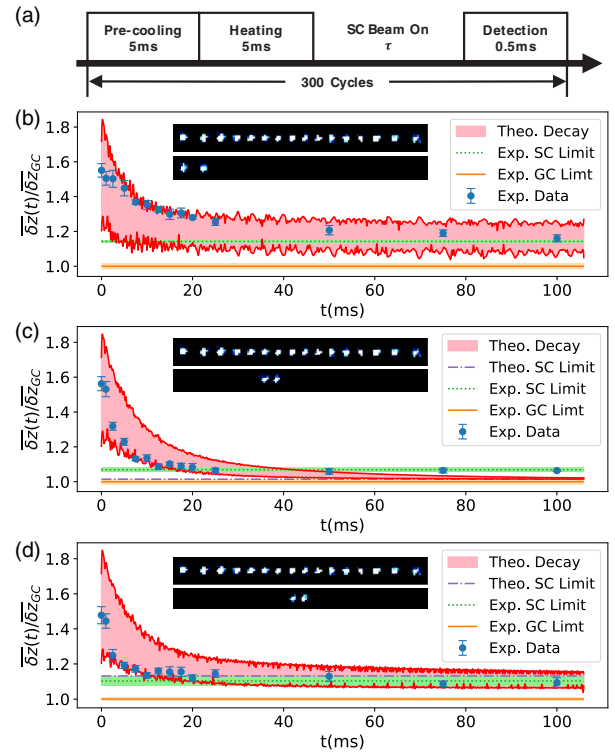

FIG. 3. (a) The experimental sequence to measure sympathetic cooling dynamics. (b)–(d) The cooling dynamics for three cooling ion pairs: (b) ions 1 and 2 on the edge, (c) the optimal ions 6 and 7, (d) ions 8 and 9 at the center. The image of the whole ion chain and that for the cooling ion pair are presented in the inset. Blue dots are the experimental data by repeating the sequence for 300 times and adding up the images together to fit the Gaussian width. The green dotted line and the orange solid line represent the sympathetic cooling limit and the global cooling limit, respectively, measured using the method of Fig. 4(a) with their widths indicating one standard deviation estimated from five repetitions. The shaded red region gives the envelope of the sympathetic cooling dynamics in theory with $\gamma_0 = 8.6$ kHz, $T_D = 3$ mK, $\kappa = 50$ mK/ s, $T_{bg} = 300$ K, and an initial temperature of $2.5 T_D$, and the purple dash-dotted line represents the theoretical cooling limit. [Not shown for (b) because there after the initial decay, the theoretical position fluctuation will rise again and will saturate for a much longer timescale.]

Material [39]), with a theoretical damping rate $\gamma_0 \approx 8.6$ kHz. As we can see, the predicted optimal cooling configuration does give the lowest axial position fluctuation even though it is slightly above the theoretical limit possibly due to the different definitions of theoretical and experimental $\overline{\delta z}$. Furthermore, we can extract a relaxation time from the measured dynamics. Here, the decay process cannot be explained by a single exponential function because there exist multiple collective modes with different cooling effects. Therefore, we define the relaxation time τ to be the time when the experimental data falls within 5% from the initial value to the steady one [measured using the sequence in Fig. 4(a)]. We hence obtain $\tau_{1,2} = 97.43$ ms, $\tau_{6,7} = 12.15$ ms, and $\tau_{8,9} = 19.86$ ms for the three cases. Again, the optimized configuration shows the best cooling effect.

Next we analyze the steady state properties, or more accurately the average behavior between 0.5 and 3.5 s as shown in Fig. 4(a), which is much longer than the typical cooling dynamics. In (b) and (c), we plot the average axial

FIG. 4. (a) The experimental sequence to measure the "cooling limit." The images for the 300 cycles are added up to Gaussian fit δz_i averaged between 0.5 and 3.5 s. (b) The experimental (red diamond) cooling limit when cooling different ion pairs (only half of the cooling pairs are measured owing to the reflection symmetry) of an $N = 16$ chain, together with the theoretical infinite-time limit (blue square) and the short-time average between 0.5 and 3.5 s (orange circle). Here, we assume that each ion is heated independently. Error bars represent one standard deviation measured by 20 repetitions. (c) The same experimental data with the theoretical results predicted by a different heating model where only the center-of-mass (COM) mode is heated. (d) The cooling effect versus the ion number when cooling the optimal ion pair. The experimental results are closer to the all-mode model than to the COM model for heating. (e) The theoretical relaxation time τ versus the ion number under three different cooling rates when cooling the optimal ion pair.

position fluctuation $\overline{\delta z}$ when a 50 nW cooling beam is located on different ion pairs of the $N = 16$ ion chain (a theoretical cooling rate $\gamma_0 \approx 11$ kHz). In (b) we compare the experimental data with the theoretical prediction based on our earlier assumption that different ions are being heated independently. The predicted steady state $\overline{\delta z}$ is low when cooling the central ions, but becomes much higher when cooling the edge and goes outside the range of the plot. This is because when cooling the edge, some of the normal modes are not efficiently cooled and thus will reach a high temperature. However, such heating is in a much longer timescale and if we compute the theoretical results between 0.5 and 3.5 s (the short-time average curve in the plot), we still get similar results as the experiment. In (c) we consider a different heating model where the random heating forces on all the ions are identical [e.g., a long-wavelength electric field noise which mainly heats the center-of-mass (COM) mode], hence $\langle \zeta_i(t)\zeta_j(t') \rangle = \delta(t - t')mk_B T_{\text{bg}}$ for all the ions not being cooled. Since all the ions have a population of $1/N$ on the COM mode, a low sympathetic cooling limit can be reached almost independent of the location of the cooling beam. However, the theoretical results between 0.5 and 3.5 s still agree with the experiment. In this sense it is difficult to distinguish these two heating models based on our experimental data.

Finally, we examine the scaling of the sympathetic cooling effect with respect to the ion number. Here, we use a 7 nW cooling beam which corresponds to $\gamma_0 \approx 3.8$ kHz. As we can see in Fig. 4(d), the measured $\overline{\delta z}/\overline{\delta z}_{\text{GC}}$, which is inversely related to the sympathetic cooling effect, increases only slowly with the ion number when cooling the optimal ion pair in the chain. We also observe that our experimental results are closer to the heating model where all the normal modes are heated rather than just the COM mode. In Fig. 4(e) we further compute the theoretical relaxation time for this "all-mode" model, using a similar definition as before by requiring the upper envelope of the theoretical curve to fall within 5% from the initial value to the steady one. Here, the relaxation time is increasing roughly linearly with the ion number, which is not surprising because the normal mode population on a fixed number of ions is decreasing as the total ion number increases. To efficiently cool a large ion crystal in the future, we will thus need to use more ions for sympathetic cooling. However, what we show here is that even a tiny fraction of ions will suffice to efficiently cool the whole crystal close to the global cooling limit.

To sum up, in this work we demonstrate multi-ion sympathetic cooling on a long ion chain. We show that, by cooling a small fraction of the ions at suitably chosen locations, the whole ion crystal can be cooled efficiently to near the global Doppler cooling limit. In this experiment we use one ion species, where, by implementing dual-type qubits [41], the laser on the cooling ions can have negligible effects on the internal states of the nearby
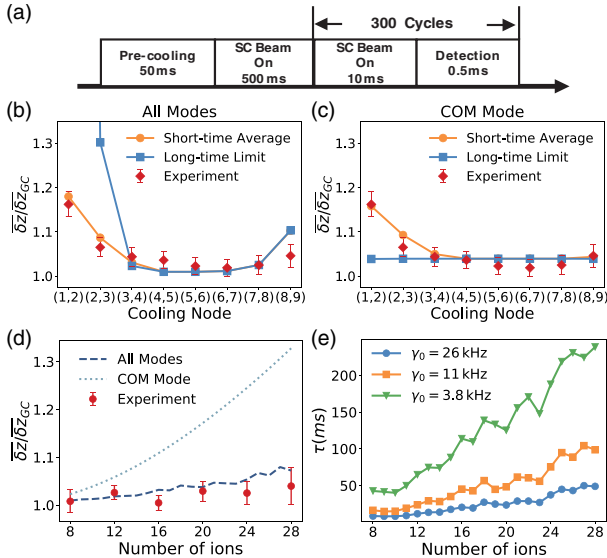
computational ions owing to the large frequency detuning. In Supplemental Material [39] we also show that the scheme can be applied in mixed-species ion chains. Hence in both cases, the sympathetic cooling beam can be applied during the quantum information processing tasks to maintain the ion crystal at a low temperature. Furthermore, our scheme can directly be generalized to 2D and 3D ion crystals with more complicated mode structures. It thus provides an important enabling step for the future large-scale ion trap quantum computing and simulation that requires long runtime.

---

[*]These authors contributed equally to this work.

[†]Present address: Department of Physics, Harvard University, Cambridge, Massachusetts 02138, USA.

[‡]zichaozhou@mail.tsinghua.edu.cn

[§]wyukai@mail.tsinghua.edu.cn

[‖]lmduan@tsinghua.edu.cn

[1] P. Wang, C.-Y. Luan, M. Qiao, M. Um, J. Zhang, Y. Wang, X. Yuan, M. Gu, J. Zhang, and K. Kim, Nat. Commun. **12**, 233 (2021).

[2] D. Leibfried, R. Blatt, C. Monroe, and D. Wineland, Rev. Mod. Phys. **75**, 281 (2003).

[3] J. I. Cirac and P. Zoller, Phys. Rev. Lett. **74**, 4091 (1995).

[4] R. Blatt and D. Wineland, Nature (London) **453**, 1008 (2008).

[5] C. Monroe and J. Kim, Science **339**, 1164 (2013).

[6] F. Mintert and C. Wunderlich, Phys. Rev. Lett. **87**, 257904 (2001).

[7] A. Khromova, C. Piltz, B. Scharfenberger, T. F. Gloger, M. Johanning, A. F. Varón, and C. Wunderlich, Phys. Rev. Lett. **108**, 220502 (2012).

[8] C. Ospelkaus, C. E. Langer, J. M. Amini, K. R. Brown, D. Leibfried, and D. J. Wineland, Phys. Rev. Lett. **101**, 090502 (2008).

[9] C. Ospelkaus, U. Warring, Y. Colombe, K. Brown, J. Amini, D. Leibfried, and D. J. Wineland, Nature (London) **476**, 181 (2011).

[10] T. P. Harty, D. T. C. Allcock, C. J. Ballance, L. Guidoni, H. A. Janacek, N. M. Linke, D. N. Stacey, and D. M. Lucas, Phys. Rev. Lett. **113**, 220501 (2014).

[11] C. J. Ballance, T. P. Harty, N. M. Linke, M. A. Sepiol, and D. M. Lucas, Phys. Rev. Lett. **117**, 060504 (2016).

[12] J. P. Gaebler, T. R. Tan, Y. Lin, Y. Wan, R. Bowler, A. C. Keith, S. Glancy, K. Coakley, E. Knill, D. Leibfried, and D. J. Wineland, Phys. Rev. Lett. **117**, 060505 (2016).

[13] I. Pogorelov, T. Feldker, C. D. Marciniak, L. Postler, G. Jacob, O. Krieglsteiner, V. Podlesnic, M. Meth, V. Negnevitsky, M. Stadler, B. Höfer, C. Wächter, K. Lakhmanskiy, R. Blatt, P. Schindler, and T. Monz, PRX Quantum **2**, 020343 (2021).

[14] L. Egan, D. M. Debroy, C. Noel, A. Risinger, D. Zhu, D. Biswas, M. Newman, M. Li, K. R. Brown, M. Cetina et al., arXiv:2009.11482.

[15] J. Zhang, G. Pagano, P. W. Hess, A. Kyprianidis, P. Becker, H. Kaplan, A. V. Gorshkov, Z.-X. Gong, and C. Monroe, Nature (London) **551**, 601 (2017).

[16] J. W. Britton, B. C. Sawyer, A. C. Keith, C.-C. J. Wang, J. K. Freericks, H. Uys, M. J. Biercuk, and J. J. Bollinger, Nature (London) **484**, 489 (2012).

[17] A. Safavi-Naini, R. J. Lewis-Swan, J. G. Bohnet, M. Gärttner, K. A. Gilmore, J. E. Jordan, J. Cohn, J. K. Freericks, A. M. Rey, and J. J. Bollinger, Phys. Rev. Lett. **121**, 040503 (2018).

[18] D. J. Wineland, C. Monroe, W. M. Itano, D. Leibfried, B. E. King, and D. M. Meekhof, J. Res. Natl. Inst. Stand. Technol. **103**, 259 (1998).

[19] C. D. Bruzewicz, J. Chiaverini, R. McConnell, and J. M. Sage, Appl. Phys. Rev. **6**, 021314 (2019).

[20] G. Milburn, S. Schneider, and D. James, Fortschr. Phys. **48**, 801 (2000).

[21] A. Sørensen and K. Mølmer, Phys. Rev. A **62**, 022311 (2000).

[22] Y.-Z. Xu, W.-D. Zhao, Y.-H. Hou, Q.-X. Mei, J.-Y. Ma, J. Wang, L. He, Z.-C. Zhou, Y.-K. Wu, and L.-M. Duan, Phys. Rev. A **102**, 063121 (2020).

[23] D. Kielpinski, C. Monroe, and D. J. Wineland, Nature (London) **417**, 709 (2002).

[24] L.-M. Duan, B. B. Blinov, D. L. Moehring, and C. Monroe, Quantum Inf. Comput. **4**, 165 (2004).

[25] L.-M. Duan and C. Monroe, Rev. Mod. Phys. **82**, 1209 (2010).

[26] C. Monroe, R. Raussendorf, A. Ruthven, K. R. Brown, P. Maunz, L.-M. Duan, and J. Kim, Phys. Rev. A **89**, 022317 (2014).

[27] S.-T. Wang, C. Shen, and L.-M. Duan, Sci. Rep. **5**, 8555 (2015).

[28] Y.-K. Wu, Z.-D. Liu, W.-D. Zhao, and L.-M. Duan, Phys. Rev. A **103**, 022419 (2021).

[29] M. Qiao, Y. Wang, Z. Cai, B. Du, P. Wang, C. Luan, W. Chen, H.-R. Noh, and K. Kim, Phys. Rev. Lett. **126**, 023604 (2021).

[30] L. Feng, W. L. Tan, A. De, A. Menon, A. Chu, G. Pagano, and C. Monroe, Phys. Rev. Lett. **125**, 053001 (2020).

[31] M. Joshi, A. Fabre, C. Maier, T. Brydges, D. Kiesenhofer, H. Hainzer, R. Blatt, and C. Roos, New J. Phys. **22**, 103013 (2020).

[32] H. Rohde, S. T. Gulde, C. F. Roos, P. A. Barton, D. Leibfried, J. Eschner, F. Schmidt-Kaler, and R. Blatt, J. Opt. B **3**, S34 (2001).

[33] B. B. Blinov, L. Deslauriers, P. Lee, M. J. Madsen, R. Miller, and C. Monroe, Phys. Rev. A **65**, 040304(R) (2002).

[34] M. D. Barrett, B. DeMarco, T. Schaetz, V. Meyer, D. Leibfried, J. Britton, J. Chiaverini, W. M. Itano, B. Jelenković, J. D. Jost, C. Langer, T. Rosenband, and D. J. Wineland, Phys. Rev. A **68**, 042302 (2003).

[35] J. P. Home, M. J. McDonnell, D. J. Szwer, B. C. Keitch, D. M. Lucas, D. N. Stacey, and A. M. Steane, Phys. Rev. A **79**, 050305(R) (2009).

[36] M. Guggemos, D. Heinrich, O. Herrera-Sancho, R. Blatt, and C. Roos, New J. Phys. **17**, 103001 (2015).

[37] J. M. Pino, J. M. Dreiling, C. Figgatt, J. P. Gaebler, S. A. Moses, M. S. Allman, C. H. Baldwin, M. Foss-Feig, D. Hayes, K. Mayer, C. Ryan-Anderson, and B. Neyenhuis, Nature (London) **592**, 209 (2021).

[38] G.-D. Lin and L.-M. Duan, Quantum Inf. Process. **15**, 5299 (2016).

[39] See Supplemental Material at http://link.aps.org/supplemental/10.1103/PhysRevLett.127.143201 for discussions about analytical cooling dynamics, about transverse motional modes, about laser beam parameters and their calibration, about cooling of mixed-species ion chains, and about the relevance of cooling timescales for practical applications, which include Ref. [40].

[40] K. Sosnova, A. Carter, and C. Monroe, Phys. Rev. A **103**, 012610 (2021).

[41] H. X. Yang, J. Y. Ma, Y. K. Wu, Y. Wang, M. M. Cao, W. X. Guo, Y. Y. Huang, L. Feng, Z. C. Zhou, and L. M. Duan, arXiv:2106.14906.